State parameter-based modelling of microstructure evolution in micro-alloyed steel during hot forming

H Buken[1] **and E Kozeschnik**[1, 2]

[1] Institute of Materials Science and Technology, Vienna University of Technology, Getreidemarkt 9, 1060 Vienna, Austria
[2] Materials Center Leoben Forschung GmbH, Roseggerstraße 12, 8700 Leoben, Austria

E-mail: heinrich.buken@tuwien.ac.at

In steel production, thermo-mechanical treatment at elevated temperatures is an inevitable step for controlling the microstructure and, thus, the mechanical-technological properties of the final product. One of the main goals in modelling microstructure evolution is the prediction of progress and interaction of hardening and softening mechanism at temperatures, where reheating, hot rolling, finish rolling and coiling are typically carried out. The main mechanisms that need to be accounted for are precipitation, grain growth, solute drag, recovery, recrystallization and phase transformation, which are to be described as functions of temperature, external loading and chemical composition of the material. In the present work, we present a new approach for dealing with these problems and apply it to the thermal and mechanical loading of microalloyed steel. Within this model, we quantitatively predict, for instance, the phenomenon of recrystallization stop in the presence of precipitation. The computational treatment is verified against experimental data from literature, where good agreement is achieved.

1. Introduction

For the case of single phase alloys that is, e.g., C- Mn- steel in the austenitic range, many constitutive laws are available that are capable of providing more or less sufficient knowledge about the static recrystallization behaviour [1]. In multiphase alloys, such as V-microalloyed steel, recrystallization kinetics can become more complicated and constitutive laws are inappropriate to describe recrystallization kinetics since a further dimension enters and influences the system: Particles cause a pinning pressure on grain boundaries. The magnitude of this Zener Drag effect is mainly determined by the precipitated phase fraction and the precipitate size but has its physical roots in the saving of energetically unfavourable total grain interface area.

Deformation provides a higher dislocation density in the material and affects the precipitation process by providing a higher nucleation site density and a higher diffusion rate in the matrix. As a consequence of this interplay of mechanisms, a description of microstructure kinetics with a single Avrami- curve [2] is not possible. Amongst many others, Medina et al. [3] show recrystallization plateaus in the presence of the common microelements Ti, Nb and V.

Modelling approaches are available in literature describing the simultaneous precipitation and recrystallization kinetics either phenomenological or physically based. Medina et al. [3] use a framework of interrelated Avrami based equations. Developing for each composition a grain size and strain dependent formula to calculate a critical maximum temperature where barely a plateau can be measured, they classify recrystallization kinetics into two regimes: a fast one with a low activation energy and a slow one where precipitates pin the grain boundaries. Nonetheless, this approach is not capable of illustrating the experimentally observed curve shapes but shows an assessment of transformation times in dependence of various material conditions and thermo-mechanical processing routes.

Zurob et al. [4] suggest a physical approach for modelling those plateaus. By simulating both, strain-induced precipitation and recrystallization kinetics, they interconnect the microstructure and precipitate evolution by the integral value of driving and retarding pressures. Once the Zener force exceeds the driving force, grain growth and recrystallization progresses come to a stop. Due to coarsening, (Ostwald ripening), the number density of precipitates decreases, they exert less influence on grain boundary movement and the Zener pressure decreases. At this point, the sum of driving pressure and retarding pressure are positive again and grains continue to grow. In this approach, Zurob et al. deliver simulation results, which show the experimentally observed curve progression.

Although some models describing coupled precipitation kinetics and microstructure evolution are available, in most approaches, either the precipitation and recrystallization kinetics are modelled implicitly, such that one set of parameters is only valid for one composition, or that the modelling of precipitation kinetics is fitted with phenomenological parameters (usually interface energies), such that the coupled model delivers microstructure results (e.g. recrystallized fraction) being in good agreement with experimental results.

In the present work and in contrast to the conventional approaches, we utilize a precipitate kinetics framework that is based on independent thermo-physical quantities (thermodynamic and kinetic databases). From these, temperature, composition and size dependent system parameters, such as interfacial energies [5–7], are computed. The state parameters are then evolved as a function of chemical composition, heat treatment and deformation regime as well as microstructure (grain size, dislocation density, etc.). For simulation of microstructure evolution, we utilize a recently developed single class recrystallization model, in which the driving forces and mobilities are computed by means of the approaches introduced subsequently. In this framework, we describe the precipitation and recrystallization interaction of low carbon steel, where the recrystallization kinetics are influenced by precipitate phases.

2. Modelling approach

2.1 Model development

The thermo-kinetic simulations of precipitation with coupled microstructure evolution are carried out with the software package MatCalc (version 6.00.007). The physical concept and functionality of the precipitate evolution, as delivered by MatCalc, is explained for the case of micro alloying elements in steel elsewhere [8,9]. To the precipitation kinetics routines of MatCalc, we couple a microstructure evolution model, which is introduced next.

The nucleation rate of recrystallized grains is modelled as

$$\dot{N}_{\mathrm{rx}} = \begin{cases} C_{\mathrm{rx}} \left(\frac{\pi}{6} \delta^2 D \right)^{-1} \exp\left(\frac{-Q_{\mathrm{rx}}}{RT}\right)(1 - X_{\mathrm{rx}}) & , \delta \geq \delta_{\mathrm{crit}} \\ 0 & , \delta < \delta_{\mathrm{crit}} \end{cases} , \qquad (1)$$

where δ is the subgrain diameter, D is the mean un-recrystallized grain diameter, C_{rx} is a calibration coefficient, Q_{rx} is an activation energy equal to the value for substitutional self-diffusion along grain boundaries, X_{rx} is the recrystallized fraction, R is the universal gas constant and T is temperature. The inverse term including the grain size and the subgrain size captures the condition that only subgrains (LAGB), which are in contact with a high-angle grain boundary can become nuclei for recrystallization as experimentally observed in ref. [10].

A second condition for nucleation is that the subgrain exceeds a critical size, δ_{crit}. This is given by the ratio of the interfacial energy of the LAGB, γ_{LB} and the driving pressure, P_D, with

$$\delta_{crit} = \frac{3\gamma_{LB}}{P_D} = \frac{3\gamma_{LB}}{0.5\mu b^2 \rho}. \quad (2)$$

The driving pressure is introduced by deformation and calculated by means of a total dislocation density, ρ, the shear modulus, μ, and the Burgers vector, b. Before nucleation takes place, the subgrain has to grow in order to overcome this critical size. On the one hand, the subgrain size is reduced by the deformation-induced dislocation that are stored in the subgrain boundaries. Nes [11] and Estrin [12] introduced the principle of similitude, where the dislocation density is correlated to a subgrainsize, δ_0, by means of a material parameter K, which is taken as starting subgrain size directly after deformation. On the other hand, the subgrain grows due to the driving pressure of capillary, where $M_{eff,LB}$ is the effective LAGB mobility.

$$\delta = \delta_0 + \dot{\delta} \cdot t = \left(\frac{K}{\sqrt{\rho}} \right) + \left(M_{eff,LB} \frac{3\gamma_{LB}}{\delta} \right) \cdot t \quad (3)$$

The growth velocity of stable nuclei, $\dot{D}_{rx}$, is expressed by the product of an effective HAGB mobility, $M_{eff, HB,}$ and the driving pressure as

$$\dot{D}_{rx} = M_{eff,HB} P_D (1 - X_{rx}). \quad (4)$$

With increasing degree of recrystallization, less deformed volume is available in which the recrystallized grains can grow into. To account for that, the growth velocity is balanced with the unrecrystallyzed volume fraction, 1-X_{rx}.

Deformation induces an increased dislocation density in the material and originates a driving pressure for recrystallization. The deformation-induced dislocation density is calculated by means of a Kocks-Mecking-type approach [13], which has been extended for static recovery by Sherstnev et al. [14].

$$\dot{\rho} = \frac{M\sqrt{\rho}}{Ab}\dot{\varphi} - 2B\frac{d_{ann}}{b}\rho M\dot{\varphi} - 2CD_{Dis}\frac{\mu b^3}{k_B T}\rho \quad (5)$$

with the Taylor factor, M, the critical dislocation annihilation distance, d_{ann}, the substitutional self-diffusion coefficient at dislocations, D_{Dis}, the Boltzmann constant, k_B, the strain rate φ, and material parameters A, B, C.

The influence of precipitates on recrystallization kinetics is incorporated via the Zener pressure, P_Z, which is given for a spatial distribution of spherical precipitates by Nes et al. [15] as

$$P_Z = \frac{3f\gamma_{HB}}{2r}, \quad (6)$$

where γ_{HB} is the HAGB energy, f is the phase fraction of precipitates and r is the precipitate radius. In contrast to most other approaches [16–18], we do not incorporate the Zener pressure into the driving force term, which may lead to a complete growth stop of the recrystallization front if the retarding force exceeds the driving force. In our treatment, we assume that the precipitates, which are arranged at the pinned grain boundary, are interconnected along a high velocity diffusion path, which allows for fast local coarsening of precipitates. Hence, the Zener pressure locally decreases and allows for a further boundary movement till a new front of precipitates is encountered, where the process of

local coarsening is repeated. We aggregate this mechanism in the form of an effective mobility, which is written as

$$M_{\text{eff}} = \begin{cases} \left(\frac{P_{\text{D}} - P_{\text{Z}}}{P_{\text{D}}}\right) M_{\text{free}} + \left(1 - \frac{P_{\text{D}} - P_{\text{Z}}}{P_{\text{D}}}\right) M_{\text{pinned}} & , P_{\text{D}} > P_{\text{Z}} \\ M_{\text{pinned}} & , P_{\text{D}} \le P_{\text{Z}} \end{cases} \qquad (7)$$

where the effective boundary mobility is calculated as superposition between a free mobility, M_{free}, in the absence of pinning, and a minimum mobility M_{pinned}, caused by precipitate pinning. This new approach provides a possibility for boundary movement even if the mean Zener pressure of the system exceeds the driving pressure for recrystallization.

2.2 Model Parameters

To verify the new model on experimental data, an evaluation of important parameters is performed first, which is summarized in table 1. Since the grain boundary mobility is a most important input parameter in our recrystallization model, we express this quantity in relation to well-assessed diffusion coefficients. Turnbull [19] suggests an upper bound for the boundary mobility, M_{TB}, with

$$M_{\text{free}} = \eta_{\text{free,HB}} \cdot M_{\text{TB}} = \eta_{\text{free,HB}} \cdot \frac{\omega D_{\text{GB}} V_{\text{m}}}{b^2 RT}, \qquad (8)$$

with the substitutional diffusion coefficient at grain boundaries, D_{GB}, the grain boundary width, ω and the molar volume of the material, V_{m}. Since atomic attachment kinetics are not accounted for within this approach, we introduce a dimensionless linear factor, $\eta_{\text{free,HB}}$, which conserves the temperature dependency of the free mobility as the ratio of the grain boundary diffusion coefficient and temperature. We adopt D_{GB} in austenite from a recent diffusion assessment of Stechauner and Kozeschnik [20]. The linear factor is adjusted to the mobility measurements of Zhou et al. [21] of plain C-Mn steel in austenite, where good agreement is achieved with a value of 1.5%.

The temperature dependency of the pinned mobility should be equal to the free mobility. Kirchner [22] suggests for precipitate coarsening at grain boundaries the same temperature dependency as Turnbull for the grain boundary mobility. Thus, we model the pinned mobility as fraction of the free mobility, which delivers with Eq. 4 a reduced growth rate in the presence of precipitates as

$$M_{\text{pinned}} = \eta_{\text{pinned,HB}} \cdot M_{\text{free}}. \qquad (9)$$

Application of this concept (section 3) shows that the mobility decreases by two orders of magnitude to 3% due to the retarding pressure exerted by the precipitates. The driving pressure for recrystallization is mainly determined by the deformation-induced dislocations and interacts with both nucleation and growth of the new microstructure. Therefore, the parameters (*A*, *B*, *C*) of the extended Kocks- Mecking model (Eq. 5) are adjusted such as to reproduce flow curve results of Hernandez et al. [23]. The observed dislocation densities do not exceed $7 \cdot 10^{14}$ m^{-2} and deliver appropriate flow stresses in the sense of the Taylor forest hardening law with input parameters similar to those mentioned in ref. [4]. The activation energy for nucleation of recrystallization (Eq. 1) mainly determines the temperature dependency of the nucleation rate. Occurring at the grain boundary, nucleation is assumed to obey the temperature dependency of grain boundary diffusion. Thus, this value is also taken from ref. [20]. The linear factor, C_{rx}, is an adjusting parameter, which balances the nucleation suppressing effect of the activation energy, but it is left constant over the range of considered materials (section 3). A collection of the elaborated parameters is given in table 1.

Table 1. Simulation input parameters

Parameter	Unit	Value	Ref.
$\eta_{free,HB}$	-	0.015	[19–21]
$\eta_{pinned,HB}$	-	0.03	This work
A	-	50	This work
B	-	5	This work
C	-	$5 \cdot 10^{-5}$	This work
Q_{rx}	kJ mol^{-1}	145	[20]
Crx	s^{-1}	1e6	This work
γ_{HB}	J m^{-2}	1.311-0.005·T	[4]
γ_{LB}	J m^{-2}	$0.5 \cdot \gamma_{HB}$	This work

3. Validation

Finally, the present microstructure model with combined precipitation kinetics is verified on experimental results from Medina et al. [24], who measured the progress of static recrystallization in diverse V-microalloyed steels. Table 2 summarizes the different compositions, starting grain sizes, D_0 and solid solution temperatures, T_{sol}, of the investigated materials.

Table 2. Considered materials at $\varepsilon = 0.35$ and $\dot{\varepsilon} = 3.62 s^{-1}$

Steel	C [wt.-%]	V [wt.-%]	N [wt.-%]	T_{sol} [°C]	D_0 [µm]
S1	0.125	0.065	0.0123	1056	167
S2	0.113	0.095	0.0144	1106	162

The two considered materials are experimentally analysed at a constant strain, ε, strain rate, $\dot{\varepsilon}$, and at different temperatures. The different precipitate solution temperatures, which are calculated with the thermokinetic software MatCalc, indicate different driving forces for precipitation. Steel S1 has a lower driving force for precipitation than steel S2 due to lower V and N contents. Therefore, the retardation of recrystallization due to precipitation is more pronounced in the more supersaturated alloy S2. At lower temperatures (below 1000°C), recrystallization starts to interact with precipitation and both steels show in that temperature range a recrystallization plateau. The more supersatured system S2 shows, in comparison to steel S1, recrystallization plateaus at lower levels of recrystallized fractions, because the Zener pressure exceeds the driving pressure for recrystallization earlier. When the retarding pressure exceeds the driving pressure, further kinetics are limited by the pinned mobility and the progress of recrystallization is decelerated. At higher temperatures ($T \geq 1000$°C), there is no interaction between precipitation and precipitation observed and both alloys show nearly the same microstructure evolution kinetics. Figure 1 depicts the results of our simulation approach in comparison to the experimental measurements of Medina et al [24].

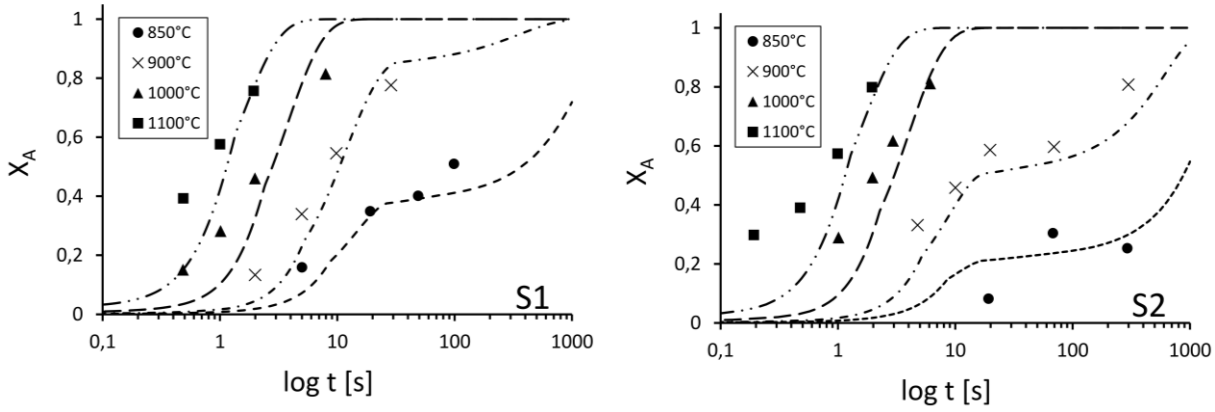

Figure 1. Recrystallization experiments vs. simulation for steel S1 and S2 at different temperatures

4. Summary

A new microstructure model is presented, where the static recrystallization process is described by the mechanisms of nucleation and growth. The growth rate of recrystallized grains is given by the product of grain boundary mobility and driving pressure. In contrast to several other models, the precipitate influence is incorporated into the mobility term and not the driving pressure term, which allows for a further growth of the recrystallized fraction even if the Zener force exceeds the driving force. The model is verified against experimental data from ref. [24], where good agreement is achieved.

5. References

[1] Beynon J and Sellars C M 1992 Modelling Microstructure and its effects during multipass hot rolling *ISIJ Int.* **32** 359–67
[2] Avrami M 1940 Kinetics of Phase Change. II Transformation-Time Relations for Random Distribution of Nuclei *J. Chem. Phys.* **8** 212–24
[3] Medina S F and Mancilla J E 1996 Static recrystallization modelling of hot deformed microalloyed steels at temperatures below the critical temperature *ISIJ Int.* **36** 1077–83
[4] Zurob H S, Brechet Y and Purdy G 2001 A model for the competition of precipitation and recrystallization *Acta Mater.* **49** 4183–90
[5] Sonderegger B and Kozeschnik E 2009 Generalized Nearest-Neighbor Broken-Bond Analysis of Randomly Oriented Coherent Interfaces in Multicomponent Fcc and Bcc Structures *Metall. Mater. Trans. A* **40** 499–510
[6] Sonderegger B and Kozeschnik E 2009 Size dependence of the interfacial energy in the generalized nearest-neighbor broken-bond approach *Scr. Mater.* **60** 635–8
[7] Sonderegger B and Kozeschnik E 2010 Interfacial Energy of Diffuse Phase Boundaries in the Generalized Broken-Bond Approach *Metall. Mater. Trans. A* **41** 3262–9
[8] Radis R and Kozeschnik E 2010 Concurrent Precipitation of AlN and VN in Microalloyed Steel *Steel Res. Int.* **81** 681–5
[9] Radis R and Kozeschnik E 2012 Numerical simulation of NbC precipitation in microalloyed steel *Model. Simul. Mater. Sci. Eng.* **20** 055010
[10] Hansen S S, Vander Sande J B and Cohen M 1980 Niobium carbide precipitation and austenite recrystallization in hot rolled microalloyed steels *Metall. Trans. A* **11A** 387–402

[11] Nes E 1997 Modelling of work hardening and stress saturation in FCC metals *Prog. Mater. Sci.* **41** 129–93
[12] Estrin Y, Tóth L S, Molinari A and Bréchet Y 1998 A dislocation-based model for all hardening stages in large strain deformation *Acta Mater.* **46** 5509–22
[13] Kocks U F and Mecking H 2003 Physics and phenomenology of strain hardening: The FCC case *Prog. Mater. Sci.* **48** 171–273
[14] Sherstnev P, Lang P and Kozeschnik E 2012 Treatment of Simultaneous Deformation and Solid- State Precipitation in Thermo-Kinetic Calculations *Eccomas 2012* 8
[15] Nes E, Ryum N and Hunderi O 1985 On the Zener drag *Acta Metall.* **33** 11–22
[16] Nes E 1976 The effect of a fine particle dispersion on heterogeneous recrystallization *Acta Metall.* **24** 391–8
[17] Humphreys F J 1997 A unified theory of recovery, recrystallization and grain growth, based on the stability and growth of cellular microstructures—II. The effect of second-phase particles *Acta Mater.* **45** 5031–9
[18] Zurob H S, Hutchinson C R, Brechet Y and Purdy G 2002 Modelling recrystallization of microalloyed austenite: effect of coupling recovery, precipitation and recrystallization *Acta Mater.* **50** 3075–92
[19] Turnbull D 1951 Theory of grain boundary migration rates *Trans. AIME* **191** 661–5
[20] Stechauner G and Kozeschnik E 2014 Assessment of substitutional self-diffusion along short-circuit paths in Al, Fe and Ni *Calphad* **47** 92–9
[21] Zhou T, O'Malley R J and Zurob H S 2010 Study of grain-growth kinetics in delta-ferrite and austenite with application to thin-slab cast direct-rolling microalloyed steels *Metall. Mater. Trans. A Phys. Metall. Mater. Sci.* **41** 2112–20
[22] Kirchner H O K 1971 Coarsening of grain-boundary precipitates *Metall. Trans.* **2** 2861–4
[23] Hernandez C A, Medina S F and Ruiz J 1996 Modelling Alloy Flow Curves in Low and Microalloyed Steels *Acta Metall.* **44** 155–63
[24] Medina S F, Mancilla J E and Hernandez C A 1993 Influence of Vanadium on the static recrystallization of austenite in microalloyed steels *J. Mater. Sci.* **28** 5317–24